

Published in final edited form as:

Acta Histochem. 2011 July ; 113(4): 428–435. doi:10.1016/j.acthis.2010.03.004.

Ectopic expression of CD74 in *Ikkβ*-deleted mouse hepatocytes

Katherine S. Koch^{a,#,*} and Hyam L. Leffert^{a,#,*}

^aHepatocyte Growth Control and Stem Cell Laboratory, Department of Pharmacology, School of Medicine, University of California at San Diego, 9500 Gilman Drive MC 0636, La Jolla, CA 92093-0636, U.S.A.

Abstract

CD74, a Type II membrane glycoprotein and MHC class II chaperone involved in antigen processing, is normally expressed by cells associated with the immune system. CD74 also forms heterodimers with CD44 to generate receptors to macrophage migration inhibitory factor (MIF), a proinflammatory cytokine. Following targeted Alb-Cre-mediated deletion of *Ikkβ* in *Ikkβ^{Δhep}* mice (*Ikkβ^{F/F}:Alb-Cre*, a strain highly susceptible to chemically-induced hepatotoxicity and hepatocarcinogenesis), CD74 is expressed abundantly by adult hepatocytes throughout liver acini, albeit more intensely in midzonal-to-centrilobular regions. By comparison, CD74 expression is not observed in *Ikkβ^{F/F}* hepatocytes, nor is it augmented in the livers of *Ikkβ^{+/+}:Alb-Cre* mice; CD74 is barely detectable in cultured embryonic fibroblasts from *Ikkβ^{-/-}* mice. Microarray profiling shows that constitutive CD74 expression in *Ikkβ^{Δhep}* hepatocytes is accompanied by significantly augmented expression of CD44 and key genes associated with antigen processing and host defense, including MHC class II I-Aα, I-Aβ, and I-Eβ chains, CIITA and CD86. Taken together, these observations suggest that *Ikkβ^{Δhep}* hepatocytes might express functional capacities for class II-restricted antigen presentation and heightened responsiveness to MIF-signaling, and also suggest further roles for intrahepatocellular IKKβ in the suppression or inactivation of molecules normally associated with the formation and differentiation of cells of the immune system.

Keywords

Hepatocytes; *Ikkβ* deletion; CD74; MHC Class II

Introduction

CD74 is recognized as the invariant chain chaperone (Ii) of MHC class II processing (Bertolino and Rabourdin-Combe, 1996). Its molecular sizes range between 31-45 kDa; the most abundant mouse isoforms, splice variants p31 and p41, are post-translationally modified with chondroitin sulfate side-chains to generate Type II membrane glycoproteins with 30 aa cytoplasmic tails (Bertolino and Rabourdin-Combe, 1996; Stumptner-Cuvelette and Benaroch, 2002). CD74 is expressed throughout the immune system by B cells, activated T cells, dendritic cells, monocytes and macrophages (Bertolino and Rabourdin-Combe, 1996; Calandra and Roger, 2003; Faure-André et al., 2008; Leng and Bucala, 2006; Lue et al., 2006; Stumptner-Cuvelette and Benaroch, 2002). In the liver, CD74 is expressed

*Corresponding authors: Tel: 858-534-2354; fax: 858-822-4184. kskoch@ucsd.edu (K.S. Koch), hleffert@ucsd.edu (H.L. Leffert).

#Both authors contributed equally to this study.

Publisher's Disclaimer: This is a PDF file of an unedited manuscript that has been accepted for publication. As a service to our customers we are providing this early version of the manuscript. The manuscript will undergo copyediting, typesetting, and review of the resulting proof before it is published in its final citable form. Please note that during the production process errors may be discovered which could affect the content, and all legal disclaimers that apply to the journal pertain.

constitutively in dendritic and Kupffer cells (Momburg et al., 1986), and in resident hepatic stellate cells (HSCs) (Maubach et al., 2007); however, except for one isolated report of a scattered sub-population of CD74-positive hepatocyte clusters (containing 1 to 5 cells) in ♀ B10.BR H-2^k mice (Momburg et al., 1986), CD74 is not expressed in hepatocytes. CD74 is also a component of heterodimeric CD74/CD44 cell surface receptors (Leng and Bucala, 2006; Lou et al., 2006) which mediate mitogenic and proinflammatory effects of macrophage migration inhibitory factor (MIF) (Calandra and Roger, 2003; Leng and Bucala, 2006; Lue et al., 2006), a 12.5 kDa cytokine secreted by a variety of T and B cells, epithelial cells, and liver Kupffer cells (Calandra and Roger, 2003; Kobayashi et al., 1999; Lan, 2008; Leng and Bucala, 2006; Lue et al., 2006). MIF exhibits intrinsic enzymatic activities; induces cyclin D1 expression, mitogenesis and NO production; and plays major roles in the pathogenesis of inflammatory disease (Javeed et al., 2008; Leng and Bucala, 2006; Swant et al., 2005). MIF expression is causally related to chronic hepatitis B virus (HBV) infection (Zhang et al., 2005), fulminant alcoholic hepatitis (Kumagi et al., 2001) and Bacille-Calmette-Guerin-primed lipopolysaccharide (LPS)-induced T cell-mediated liver failure (BLTLF) (Kobayashi et al., 1999). Anti-MIF antisera block BLTLF (Kobayashi et al., 1999) and attenuate experimentally-induced murine colitis (de Jong et al., 2001); anti-sense MIF cDNA attenuates LPS-induced liver injury (Iwaki et al., 2003); and MIF knockout mice are protected from concanavalin A (ConA), LPS- and acetaminophen-induced liver injuries (Bourdi et al., 2002; Bozza et al., 1999; Nakajima et al., 2006). CD74 also is cleaved by regulated intracellular proteolysis (RIP) to form a 10-kDa cytoplasmic polypeptide fragment which migrates into the nucleus and activates nuclear factor kappa B (NF-κB) expression (Becker-Herman et al., 2005). However, the relationship between CD74 and NF-κB in liver disease remains unclear.

To understand how NF-κB, a transcription factor that plays anti-inflammatory and protective roles in hepatotoxic injury (Heyninck et al., 2003) and mediates liver disease, we have investigated an hepatocyte-targeted mouse strain (*Ikkβ^{Ahep}*) with Cre recombinase-mediated deletions of IκB kinase β (*Ikkβ*) exon 3 (Maeda et al., 2003). IKKβ, a subunit of the IκB Kinase (IKK) complex, is required for activation of NF-κB (Ghosh and Karin, 2002; Heyninck et al., 2003). *Ikkβ^{Ahep}* mice exhibit defective activation of NF-κB and survival genes, and enhanced susceptibility to hepatotoxins (Maeda et al., 2003, 2005). Following ConA- or LPS+Galactosamine-induced inflammation, *Ikkβ^{Ahep}* mice exhibit heightened susceptibility to liver failure, resulting partly from tumor necrosis factor (TNF)α-activation of TNF receptor 2 (TNFR2; Maeda et al., 2003), and from increased reactive oxygen species (ROS) formation. ROS inhibits mitogen activated protein kinase (MAPK) phosphatases and sustains c-JUN nuclear kinase 1 (JNK1) activation (Kamata et al., 2005; Maeda et al., 2003). Following treatment with diethylnitrosamine (DEN), *Ikkβ^{Ahep}* mice exhibit increased susceptibility to hepatocellular carcinoma (HCC), resulting partly from cytokine-driven NF-κB activation-independent compensatory hepatocyte proliferation (Laurent et al., 2005; Maeda et al., 2005); from sustained JNK1 activation, accompanied by necrotic hepatocellular interleukin (IL)-1α release which activates IL-1 receptors in Kupffer cells and IL-6 secretion (Sakurai et al., 2008); and, as described most recently, from intrinsic *Ikkβ^{Ahep}* hepatocellular growth advantages (Koch et al., 2009).

Neither CD74 nor MIF has been linked to the pathophysiological responses of *Ikkβ^{Ahep}* hepatocytes, or to *Ikkβ*-deletion in other cells in other IKKβ-deficient mice (Chen et al., 2006; Malato et al., 2008). However, CD74 is required for major histocompatibility (MHC) class II antigen processing (Bertolino and Rabourdin-Combe, 1996); and MIF has wide-ranging effects on hepatic inflammation, infection and tumor progression (Bourdi et al., 2002; Bozza et al., 1999; Calandra and Roger, 2003; de Jong et al., 2001; Iwaki et al., 2003; Nakajima et al., 2006; Zhang et al., 2005). In addition, because the proinflammatory effects elicited by the CD74/CD44 MIF receptor, like those by TNFR2 (Maeda et al., 2003), require

sustained kinase activation (Leng and Bucala, 2006), we investigated constitutive CD74 expression in *Ikkβ^{Δhep}* and *Ikkβ^{F/F}* mice.

Surprisingly, we find that *Ikkβ^{Δhep}* hepatocytes express CD74, whereas *Ikkβ^{F/F}* hepatocytes do not. In addition, as assessed by microarray profiling, the hepatocellular CD74-positive phenotype is accompanied by the expression of large numbers of genes normally associated with immune system processing and host defense mechanisms, including MHC class II I-A α , I-A β , and I-E β chains, CD44, the transcriptional coactivator of MHC class II expression CIITA (Ting and Trowsdale, 2002), and coactivator CD86. These observations suggest that targeted *Ikkβ* deletion confers several unexpected and unusual immunologic phenotypes in hepatocytes which, if functionally active, might have significant implications for both the pathophysiology of liver disease and the regulation of animal cell differentiation.

Materials and Methods

Animals and cell culture

C57BL/6, *Ikkβ^{+/+}:Alb-Cre*, *Ikkβ^{F/F}* and *Ikkβ^{F/F}:Alb-Cre* (referred to as *Ikkβ^{Δhep}*) mice were bred at UCSD (La Jolla, CA), maintained and sacrificed according to NIH guidelines (Koch et al., 2009; Maeda et al., 2003). Protocols used in all animal studies were approved by the UCSD IACUC animal ethics committee. Mouse embryonic fibroblasts (MEFs) from *Ikkβ^{-/-}* embryos were cultured under standard conditions (Chen et al., 2006).

Isolation and analyses of primary hepatocytes, tissues and macromolecules

Freshly isolated hepatocytes and liver tissues were harvested from adult mice; DNA, RNA and proteins were isolated from hepatocytes, liver tissues and MEFs as described elsewhere (Chen et al, 2006; Koch et al., 2009; Maeda et al., 2003). *Ikkβ* deletion and genotyping tests were performed by polymerase chain reaction (PCR) using DNA from tails, livers and cultured hepatocytes and MEFs (Chen et al, 2006; Koch et al., 2009; Maeda et al., 2003). RNA and DNA were sized by gel-electrophoresis (Koch et al., 2009).

Microarray profiling

Animals were sacrificed and tissues harvested at 5-6 weeks of age. RNA samples were labeled and hybridized by standard procedures (Feng et al., 2007) using two Illumina WG-6 V2 mouse bead-chips (San Diego, CA, cat. #BD 201-0202) in the UCSD BIOGEM Core (<http://microarrays.ucsd.edu/>). Each chip carried 6 microarrays housing 47,000 oligonucleotide targets representing ~5,000 genes/array (see: Fig. 1). Data were normalized and grouped (using the gene ontology databases from the Gene Ontology Consortium [www.genego.org] including pathways from KEGG, Biocarta, and Proteinlounge databases), and analyzed for statistical significance (Feng et al., 2007). Quantitative variation among data samples for individual genes was <1-2%. The original data (see Tables 1 and 2) have been entered into the NCBI GEO Repository (<http://www.ncbi.nlm.nih.gov/projects/geo/query/acc.cgi?acc=GSE15476>); a sample of selected data in Table 1 has been presented elsewhere (Koch and Leffert, 2010). For GenBank details and probes employed for these analyses, see the Illumina Reference Chip file, MouseWG-6_V2_0_R2_11278593_A (<http://www.switchtoi.com/annotationfiles.ilmn>).

Western blots

Animals were sacrificed and tissues harvested at 58 and 48 days (see Figures 2A [lanes 3-6] and 2B [lanes 1-4], both panels, respectively), and at 125 days (see Figure 2B [lanes 5 and 6], both panels) of age. Liver extracts (30 μ g proteins/lane) and cultured MEF extracts (40 μ g) were analyzed on non-reducing prefabricated 10% SDS-PAGE gels (Invitrogen, Carlsbad, CA; Koch et al., 2009). Proteins were transferred to nitrocellulose membranes

using an Xcell II blot module (Invitrogen, Carlsbad, CA). Membranes were incubated overnight with either primary (‘1°’) rat anti-mouse CD74 antibody (clone In-1, BD Biosciences Pharmingen, San Diego, CA, catalog (cat.) #555317) or with matched rat IgG2b, κ isotype control (BD Biosciences Pharmingen, San Diego, CA, cat. #553986), washed, incubated 2 hr with secondary (‘2°’) horse radish peroxidase (HRP)-conjugated goat anti-rat IgG (H+L) (Pierce, ThermoScientific, Rockford, IL, cat. #31470), washed, and incubated 1 hr with ECL-Western-Blotting substrate according to the supplier’s instructions (Pierce, ThermoScientific, Rockford, IL, cat. #32106). Loading control blots using identical extracts were performed with anti-GRP94 (gp96) antibody (Santa Cruz Biotechnologies, Santa Cruz, CA, cat. #sc-71182). Chemiluminescence was visualized by 5-30 sec exposure to Amersham ECL-Hyperfilm (GE Healthcare Biosciences, Piscataway, NJ, cat. #28-9068-36). Results of Western blots were obtained from different extracts from two independent experiments.

Immunohistochemistry

Animals were sacrificed and liver tissues (portions of the right lobe) harvested at 58 days of age. Thin sections (5 μ m) of paraffin blocks of fixed tissues (4% paraformaldehyde in PBS, 24 hr at 4 °C), and routine hematoxylin and eosin (H&E) stained sections were prepared by standard automated procedures in the UCSD Cancer Center Histology Core (<http://cancer.ucsd.edu/Research/Shared/histology.asp>). For immunohistochemical staining, endogenous peroxidase activity was blocked in deparaffinized sections with 3% H₂O₂. Sections were pretreated with Retrieval A* according to the supplier’s protocol (BD Pharmingen, San Diego, CA, cat. #550524), followed by 10% fetal bovine serum (Gibco Invitrogen, Carlsbad, CA) to block non-specific binding. Slides were washed, and incubated with 1° anti-CD74 antibody or with matched isotype control rat IgG2b, κ antibody at final concentrations of 5 μ g/mL for 1 hr at 21°C. Slides were washed, treated with biotinylated goat 2° anti-rat Ig (BD Pharmingen, San Diego CA, cat. #51-7605KC) for 30 min at 21 °C, washed and treated with Streptavidin-HRP (BD Pharmingen, San Diego CA, cat. #551013) for 30 min at 21 °C. After further washing, the slides were incubated with diaminobenzidine solution (BD Pharmingen, San Diego CA, cat. #551013) for 0.5-5 min (or, as needed), washed, counterstained in Meyer’s hematoxylin, dehydrated and coverslipped. Digital images and information (available on request) were acquired with NIS-Elements F 2.30 software, by Nikon DS-Ri1 camera, from Nikon Diaphot with 20 \times (Fig. 3) or 4 \times (Fig. 4) objectives. Independent immunohistochemical staining experiments utilizing sections from at least two animals of each genotype were performed multiple times.

Results

Microarray profiling shows upregulation of immune phenotypic expression in *Ikk β ^{Δhep}* hepatocytes

Liver tissue and isolated hepatocytes from both genotypes (four separate samples) were compared to see whether profiling differences would be more or less enriched in hepatocytes compared to total liver. RNA sizing and DNA genotyping were performed prior to profiling studies. Intact RNA of high quality (Fig. 1A), and PCR products consistent with wild type and *Ikk β* -deleted genomes were observed (Fig. 1B) (Maeda et al., 2003). Microarray hybridizations were performed in triplicate with formatting as diagrammed in Figure 1C.

Key findings in the largest expression group (‘Biological Process’) are shown for freshly isolated livers and freshly isolated hepatocytes in Tables 1 and 2, respectively. Two functional sub-families topped both lists at very high levels of statistical significance (albeit in reverse order): **liver** (immune system process, $p \sim 6.5 \times 10^{-28}$; defense response, $p \sim 2 \times 10^{-27}$); **hepatocytes** (defense response, $p = 1.4 \times 10^{-21}$; immune system process, $p \sim 1.2 \times$

10^{-18}). Examination of the 6-19 genes topping these lists showed that all were expressed at relatively higher levels in *Ikk β^{Ahep}* samples, except for two which were higher in *Ikk $\beta^{F/F}$* liver tissue (histocompatibility 2, blastocyst H2-B1 [both sub-families]) and one which was apparently higher in *Ikk $\beta^{F/F}$* hepatocytes (CD163 antigen [defense response]).

Enhanced CD74 expression in *Ikk β^{Ahep}* samples ranked highest throughout; CD74 was enriched ~38-fold in isolated *Ikk β^{Ahep}* hepatocytes, and ~8-fold in *Ikk β^{Ahep}* liver tissue (a 5-fold enrichment following hepatocyte isolation; see both Tables 1 and 2). Profiling also indicated that additional immune process and defense genes were significantly upregulated >4-10-fold in *Ikk β^{Ahep}* hepatocytes, including MHC class II I-A α , I-A β , and I-E β chains, CD44, Cxcl9, guanylate nucleotide binding proteins 1-3, TAP, Tlr2, interferon gamma (IFN- γ) inducible protein 47 and IFN- γ regulatory factor 1 (see both Tables 1 and 2). Direct inspection of the microarray data also revealed augmented expression levels of *Ikk β^{Ahep}* hepatocyte CIITA, STAT1, cathepsin S, co-activator CD86 and programmed death ligand-1 (PD-L1) (> 6-, 5.4-, 3.6-, 2- and 5.5-fold, respectively), all significantly greater than isolated liver tissue. As shown in Table 3, the available data from microarray comparisons between *Ikk β^{Ahep}* hepatocytes and *Ikk $\beta^{-/-}$* MEFs revealed few similarities (Chen et al., 2006).

Ectopic expression of CD74 proteins is upregulated in *Ikk β^{Ahep}* hepatocyte extracts

Four specific bands ($M_r \sim 31, 35, 41$ kDa, and a 10-12 kDa doublet) were detected in *Ikk β^{Ahep}* liver extracts by antibody specific to cytosolic CD74 epitopes (Figs. 2A and 2B [left panels]). CD74-specific bands were not seen in similar extracts probed with isotype control antibody (Figs. 2A and 2B [right panels]). Band intensities were similar in σ and ϕ samples; the relative intensities of p31 were ~2.5-fold higher than p41 as expected (Bertolino and Rabourdin-Combe, 1996). In contrast, some (p31 and p41) but not all (p35, p45 and the 10-12 kDa doublet) CD74-specific bands were detectable at significantly lower levels in *Ikk $\beta^{F/F}$* liver extracts (Figs. 2A and 2B [left panels]); these bands were likely due to CD74 expressed by non-parenchymal cells (NPCs) in the intact livers (Fig. 3). The finding of CD74-specific expression in *Ikk β^{Ahep}* liver extracts was not an artifact of albumin promoter-driven Cre expression, as CD74 expression levels in liver extracts from *Ikk $\beta^{+/+}$:Alb-Cre* mice were similar to those from *Ikk $\beta^{F/F}$* mice, with no detectable p35, p45, or 10-12 kDa doublet (Fig. 2B).

As expected from profiling (Chen et al., 2006), CD74 was undetectable in wildtype MEF extracts whereas extracts from *Ikk $\beta^{-/-}$* MEFs variably expressed very low levels of p31 and p41 bands but undetectable levels of p35 or the 10-12 kDa doublet (Figs. 2A and 2B [left panels]). The significance of these observations is currently unclear.

Ectopic and specific expression of CD74 is observed *in situ* in *Ikk β^{Ahep}* hepatocytes

To localize hepatic CD74 expression, livers from σ C57BL/6, and σ and ϕ *Ikk $\beta^{F/F}$* and *Ikk β^{Ahep}* mice were analyzed by routine histology and immunohistochemistry. In all cases, the same 1 $^\circ$ antibody used for Western blots was employed; with respect to *Ikk $\beta^{F/F}$* and *Ikk β^{Ahep}* mice, portions of the same tissue samples used for Western blots (Fig. 2A) were fixed for histochemistry (Figs. 3 and 4).

Normal histology was observed by H&E staining of C57BL/6 liver (Fig. 3, row 1). As expected (Maubach et al., 2007; Momburg et al, 1986), specific CD74 staining was observed in NPCs bordering a portal triad, and also scattered sparsely throughout the liver. In contrast, specific staining was not observed either in hepatocytes, or in cells bordering the central vein, or in sections incubated with isotype control antibody (Fig. 3, row 1). The faint CD74-positive p31 and p41 bands on Western blots of liver extracts from *Ikk $\beta^{+/+}$:Alb-Cre* and *Ikk $\beta^{F/F}$* mice (Figs. 2A and 2B) may reflect NPC staining. Further work is needed for

precise identification of NPCs, whether dendritic, HSC, Kupffer, sinusoidal endothelial and/or biliary ductular epithelial cells, which are responsible for this CD74-positive staining.

As shown in Fig. 3 (rows 2-5), H&E staining showed no morphological differences between *Ikkβ^{Ahep}*, and control *Ikkβ^{F/F}*, ♀ or ♂ livers. However, intense CD74 staining was observed in virtually all *Ikkβ^{Ahep}* hepatocytes throughout liver acini and regardless of gender. Specific CD74 staining in *Ikkβ^{Ahep}* hepatocytes was associated with cytoplasmic and with membrane sites. In contrast, although scattered periportal and acinar staining was observed in NPCs, specific CD74 staining was undetectable in *Ikkβ^{F/F}* hepatocytes. No CD74 staining was observed in any liver sections incubated with isotype control antibody (Fig. 3) or in the absence of 1° antibody (data not shown).

By observation of liver sections at lower magnification (Fig. 4), specific CD74 staining in *Ikkβ^{Ahep}* livers appeared to be more intense in hepatocytes bordering central veins, and to decrease slightly and gradually in intensity from centrilobular to periportal zones.

Discussion

Immunohistochemical, microarray profiling, and Western blot findings show ectopic and gender-independent expression of major, minor and putatively processed CD74 isoforms in hepatocytes deleted in *Ikkβ* (*Ikkβ^{Ahep}*). Immunohistochemistry suggests that antibody-specific CD74 expression occurs in all hepatocytes, as might be expected from *Ikkβ*-deletion analyses indicating no undetected product in a population of isolated *Ikkβ^{Ahep}* hepatocytes (Maeda et al., 2003; Koch et al., 2009); however, the isoform(s) responsible for the observed immunochemical reactivities have not been specifically identified. The prominent 35 kDa band in *Ikkβ^{Ahep}* liver extracts might represent another CD74 murine isoform, so far unreported; the nature of the 45 kDa band observed in younger but not older mice (compare Fig. 2A with Fig. 2B) is unclear. The 10-12 kDa doublet, also observed in spleens from *Ikkβ^{+/+}:Alb-Cre* mice (Fig. 2B [left panel]), might be a form of RIP-processed CD74 (Becker-Herman et al., 2005); if functional, this might account for residual NF-κB activity in *Ikkβ^{Ahep}* hepatocytes (Maeda et al., 2003).

The occurrence of multiple isoforms complicates interpretation of immunohistochemical observation of enriched midzonal-to-centrilobular localization of hepatocellular CD74, since site-enrichment could be due either to increased expression of all or selected isoforms, or to increased availability of antigenic sites of one or more equally abundant isoforms. Alternatively, owing to the relatively short paraformaldehyde fixation time, and to subsequent variably effective antigen retrieval steps, zonal staining intensity differences might reflect differential fixation of antigenic sites accessible to the anti-CD74 antibody employed. Whereas longer fixation times (> 24 hr) clearly reduce antigen detection (data not shown), zonal differences were still visible. Therefore, because the zonal differentiation of hepatocytes is responsible for many functional attributes of liver under both normal, and pathological conditions, further experiments are needed to clarify these observations as well as to eliminate other possible fixation artifacts.

Although the upregulation of CD74 expression in hepatocytes appears to be a consequence of targeted hepatocellular deletion of *Ikkβ* in *Ikkβ^{Ahep}* mice, *Ikkβ* deletion alone is not a uniformly sufficient condition of CD74 upregulation, because *Ikkβ^{-/-}* MEFs express only barely detectable levels of CD74, as revealed by Western blots (Fig. 2), and none by RNA profiling (Chen et al., 2006). While the mechanisms responsible for ectopic hepatocellular CD74 expression remain to be determined, they do not appear to be random or isolated. This conclusion is supported by liver micorarray profiling results which reveal, with very high statistical significance, that augmented CD74 expression in *Ikkβ^{Ahep}* hepatocytes is

concomitant with enriched expression of two large families of immune system-related genes, among them CD44, MHC class II I-A α , I-A β , and I-E β chains, CIITA and PD-L1 mRNAs, the functions of which are involved in antigen processing, host defense and liver tolerance (Tiegs and Lohse, 2009). This enrichment is selectively greater in isolated hepatocytes compared to that in unfractionated liver extracts. Although further work is needed to show the translation of these mRNAs directly and to characterize the cellular locations of these putatively translated proteins, these additional findings are surprising and intriguing because the expression of all five of these molecules, like CD74, is usually restricted to lymphoid (Abbas et al., 2010; Rafi-Janajreh et al., 1998) and NPCs (Tiegs and Lohse, 2009).

The collective, and significantly augmented, expression of CD74 and these two gene families in *Ikk β ^{Δhep}* hepatocytes suggests several interrelated hypotheses about ectopic immunologic functions and susceptibility to HCC in these mice, as discussed elsewhere (Koch and Leffert, 2010).

Acknowledgments

This work was supported by NIH (CA113602, AI067354) and the Superfund Basic Research Program (P42ES010337). Breeding colonies were started with mice generously supplied by M. Karin (UCSD), whom we also thank for the suggestion to examine *Ikk β ^{+/+}:Alb-Cre* mice. We thank K. Juson, M. Zhang and A. Elbehti for technical assistance; Anne Chang (UCSD, Karin Laboratory) for wildtype and *Ikk β ^{-/-}* MEFs and *Ikk β ^{+/+}:Alb-Cre* mice; and R. Sasik (UCSD BIOGEM Core) for statistical analyses and organization of microarray profiling data.

References

- Abbas, AK.; Lichtman, AH.; Pillai, S. Cellular and Molecular Immunology. Updated 6th. Philadelphia: Saunders Elsevier; 2010.
- Becker-Herman S, Arie G, Medvedovsky H, Kerem A, Shachar I. CD74 is a member of the regulated intramembrane proteolysis-processed protein family. *Mol Biol Cell*. 2005; 11:5061–9. [PubMed: 16107560]
- Bertolino P, Roubourdin-Combe C. The MHC class II-associated invariant chain: a molecule with multiple roles in MHC class II biosynthesis and antigen presentation to CD4+ T cells. *Crit Rev Immunol*. 1996; 16:359–79. [PubMed: 8954255]
- Bozza M, Satskar AR, Lin G, Lu B, Humbles AA, Gerard C, et al. Targeted disruption of migration inhibitory factor gene reveals its critical role in sepsis. *J Exp Med*. 1999; 189:341–6. [PubMed: 9892616]
- Bourdi M, Reilly TP, Elkahlon AG, George JW, Pohl LR. Macrophage migration inhibitory factor in drug induced liver injury: a role in susceptibility and stress responsiveness. *Biochem Biophys Res Commun*. 2002; 294:225–30. [PubMed: 12051698]
- Calandra T, Roger T. Macrophage migration inhibitory factor: a regulator of innate immunity. *Nature Reviews Immunology*. 2003; 3:791–800.
- Chen F, Lu Y, Castranova V, Li Z, Karin M. Loss of Ikkbeta promotes migration and proliferation of mouse embryo fibroblast cells. *J Biol Chem*. 2006; 281:37142–9. [PubMed: 16966325]
- de Jong YP, Abadia-Molina AC, Satskar AR, Clarke K, Rietdijk ST, Faubion WA, et al. Development of chronic colitis is dependent on the cytokine MIF. *Nat Immunol*. 2001; 2:1061–6. [PubMed: 11668338]
- Faure-André G, Vargas P, Yuseff MI, Heuzé M, Diaz J, Lankar D, et al. Regulation of dendritic cell migration by CD74, the MHC class II-associated invariant chain. *Science*. 2008; 322:1705–10. [PubMed: 19074353]
- Feng Z, Davis DP, Sásik R, Patel HH, Drummond JC, Patel PM. Pathway and gene ontology based analysis of gene expression in a rat model of cerebral ischemic tolerance. *Brain Res*. 2007; 1177:103–23. [PubMed: 17916339]
- Ghosh S, Karin M. Missing pieces in the NF- κ B puzzle. *Cell*. 2002; 109:S81–S96. [PubMed: 11983155]

- Heyninck K, Wullaert A, Beyaert R. Nuclear factor- κ B plays a central role in tumour necrosis factor-mediated liver disease. *Biochem Pharmacol.* 2003; 66:1409–15. [PubMed: 14555215]
- Iwaki T, Sugimura M, Nishihira J, Matsuura T, Kobayashi T, Kanayama N. Recombinant adenovirus vector bearing antisense macrophage migration inhibitory factor cDNA prevents acute lipopolysaccharide induced liver failure in mice. *Lab Invest.* 2003; 83:561–70. [PubMed: 12695559]
- Javeed A, Zhao Y, Zhao Y. Macrophage-migration inhibitory factor: role in inflammatory diseases and graft rejection. *Inflamm Res.* 2008; 57:45–50. [PubMed: 18288453]
- Kamata H, Honda S, Maeda S, Chang L, Hirata H, Karin M. Reactive oxygen species promote TNF α induced death and sustained JNK activation by inhibiting MAP kinase phosphatases. *Cell.* 2005; 120:649–61. [PubMed: 15766528]
- Kobayashi S, Nishihira J, Watanabe S, Todo S. Prevention of lethal acute hepatic failure by antimacrophage migration inhibitory factor antibody in mice treated with bacille Calmette-Guerin and lipopolysaccharide. *Hepatology.* 1999; 29:1752–9. [PubMed: 10347118]
- Koch KS, Leffert HL. Hypothesis: Targeted *Ikk β* deletion upregulates MIF signaling responsiveness and MHC class II expression in mouse hepatocytes. *Hepatic Medicine: Evidence and Research.* 2010 In press.
- Koch KS, Maeda S, He G, Karin M, Leffert HL. Targeted deletion of hepatocyte *Ikk β* confers growth advantages. *Biochem Biophys Res Commun.* 2009; 380:349–54.
- Kumagi T, Akbar F, Horiike N, Onji M. Increased serum levels of macrophage migration inhibitory factor in alcoholic liver diseases and their expression in liver tissues. *Clin Biochem.* 2001; 34:189–93. [PubMed: 11408016]
- Lan HY. Role of macrophage migration inhibition factor in kidney disease. *Nephron Exp Nephrol.* 2008; 109:e79–e83. [PubMed: 18663334]
- Laurent S, Horsmans Y, Stärkel P, Leclercq I, Sempoux C, Lambotte L. Disrupted NF- κ B activation after partial hepatectomy does not impair hepatocyte proliferation in rats. *World J Gastroenterol.* 2005; 11:7345–50. [PubMed: 16437640]
- Leng L, Bucala R. Insight into the biology of macrophage migration inhibitory factor (MIF) revealed by the cloning of its cell surface receptor. *Cell Res.* 2006; 16:162–8. [PubMed: 16474429]
- Lue H, Kapurniotu A, Fingerle-Rowson G, Roger T, Leng L, Thiele M, et al. Rapid and transient activation of the ERK MAPK signaling pathway by macrophage migration inhibitory factor (MIF) and dependence on JAB1/CSN5 and Src kinase activity. *Cell Signal.* 2006; 18:688–703. [PubMed: 16122907]
- Maeda S, Chang L, Li ZW, Luo JL, Leffert H, Karin M. IKK β is required for prevention of apoptosis mediated by cell-bound but not by circulating TNF α . *Immunity.* 2003; 19:725–37. [PubMed: 14614859]
- Maeda S, Kamata H, Luo JL, Leffert H, Karin M. IKK β couples hepatocyte death to cytokine-driven compensatory proliferation that promotes chemical hepatocarcinogenesis. *Cell.* 2005; 121:977–90. [PubMed: 15989949]
- Malato Y, Sander LE, Liedtke C, Al-Masaoudi M, Tacke F, Trautwein C, et al. Hepatocyte-specific inhibitor-of- κ B-kinase deletion triggers the innate immune response and promotes earlier cell proliferation during liver regeneration. *Hepatology.* 2008; 47:2036–50. [PubMed: 18393321]
- Maubach G, Lim MC, Kumar S, Zhuo L. Expression and upregulation of cathepsin S and other early molecules required for antigen presentation in activated hepatic stellate cells upon IFN- γ treatment. *Biochim Biophys Acta.* 2007; 1773:219–31. [PubMed: 17178165]
- Momburg F, Koch N, Möller P, Moldenhauer G, Butcher GW, Hämmerling GJ. Differential expression of Ia and Ia-associated invariant chain in mouse tissues after in vivo treatment with IFN- γ . *J Immunol.* 1986; 136:940–8. [PubMed: 3079804]
- Nakajima H, Takagi H, Horiguchi N, Toyoda M, Kanda D, Otsuka T, et al. Lack of macrophage migration inhibitory factor protects mice against concanavalin A-induced liver injury. *Liver Int.* 2006; 26:346–51. [PubMed: 16584398]
- Rafi-Janajreh AQ, Nagarkatti PS, Nagarkatti M. Role of CD44 in CTL and NK cell activity. *Front Biosci.* 1998; 3:d665–71. [PubMed: 9634546]

- Sakurai T, He G, Matsuzawa A, Yu GY, Maeda S, Hardiman G, et al. Hepatocyte necrosis induced by oxidative stress and IL-1 α release mediate carcinogen-induced compensatory proliferation and liver tumorigenesis. *Cancer Cell*. 2008; 14:156–65. [PubMed: 18691550]
- Stumptner-Cuvelette P, Benaroch P. Multiple roles of the invariant chain in MHC class II function. *Biochim Biophys Acta*. 2002; 1542:1–13. [PubMed: 11853874]
- Swant JD, Rendon BE, Symons M, Mitchell RA. Rho GTPase-dependent signaling is required for macrophage migration inhibitory factor-mediated expression of cyclin D1. *J Biol Chem*. 2005; 280:23066–72. [PubMed: 15840582]
- Tiegs G, Lohse AW. Immune tolerance: What is unique about the liver. *J Autoimmun*. Aug 28.2009 Epub ahead of print.
- Ting JP, Trowsdale J. Genetic control of MHC class II expression. *Cell*. 2002; 109:S21–33. [PubMed: 11983150]
- Zhang HY, Nanji AA, Luk JM, Huang XR, Lo CM, Chen YX, et al. Macrophage migration inhibitory factor expression correlates with inflammatory changes in human chronic hepatitis B infection. *Liver Int*. 2005; 25:571–9. [PubMed: 15910495]

Abbreviations

Alb	refers to albumin-specific gene promotor
BLTLF	Bacille–Calmette–Guerin-primed lipopolysaccharide-induced T cell-mediated acute liver failure
ConA	lectin concanavalin A
CIITA	transcriptional coactivator of MHC class II expression
Cre	cre recombinase
DEN	diethylnitrosamine
HBV	hepatitis B virus
HCC	hepatocellular carcinoma
H&E	hematoxylin and eosin
HRP	horse radish peroxidase
HSC	hepatic stellate cell
IFN-γ	interferon γ
Ii	invariant chain CD74 chaperone
IKK	I κ B complex
IKKβ	protein kinase subunit of IKK
<i>Ikkβ^{F/F}</i>	mouse strain carrying Cre-recombinase sites (F/F) spanning <i>Ikkβ</i> exon 3
<i>Ikkβ^{Δhep}</i>	mouse strain <i>Ikkβ^{F/F}:Alb-Cre</i> , specifically deleted in hepatocyte <i>Ikkβ</i>
IL	interleukin
JNK	c-JUN nuclear kinase
LPS	lipopolysaccharide
MAPK	mitogen-activated protein kinase
MEFs	mouse embryonic fibroblasts
MHC	major histocompatibility
MIF	macrophage migration inhibitory factor

NPC	non-parenchymal cell
NF-κB	nuclear factor kappa B
PD-L1	programmed death ligand
RIP	regulated intramembrane proteolysis
ROS	reactive oxygen species
STAT	signal transducers and activator of transcription
TNF	tumor necrosis factor
TNFR2	tumor necrosis factor receptor 2

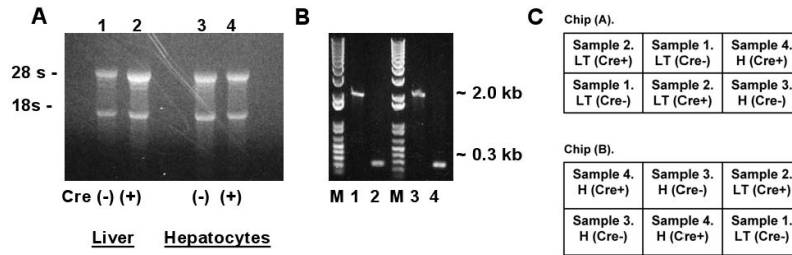
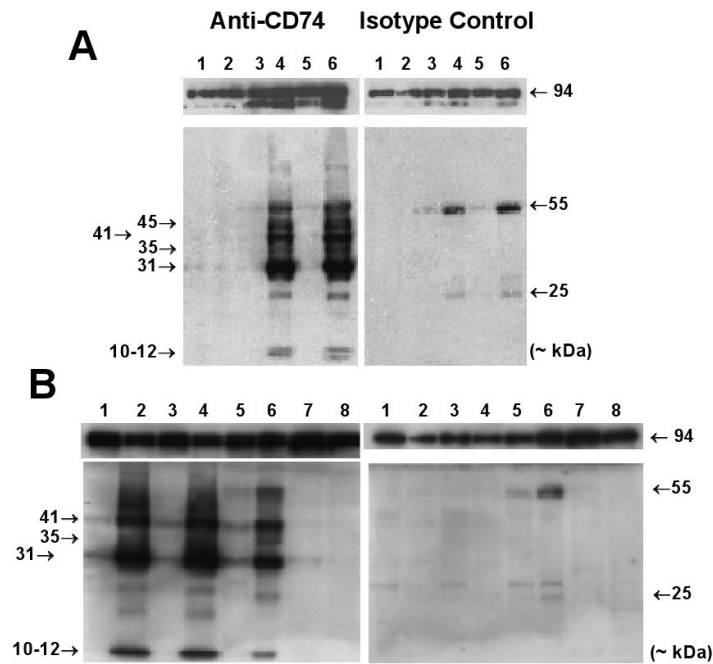


Figure 1.

Analysis of RNA and DNA from male Cre(-) *Ikkβ^{F/F}* and Cre(+) *Ikkβ^{Ahep}* mouse livers and freshly isolated hepatocytes used for microarray profiling. (A) EtBr-stained RNA-sizing gel. (B) Deletion analysis. EtBr-stained DNA-sizing gel. Genotyping for deletion confirmation was performed by PCR using standard primers (Koch et al., 2009). M, size markers (bps); lanes #1-#4 as in panel (A); Cre(-) ~2-kb, Cre(+) ~0.3-kb. (C) Hybridization format: chips 1 (A) and 2 (B). Each RNA sample (liver tissue [LT], or isolated hepatocytes [H]) was obtained from a separate mouse: Samples #1 and #2, Cre(-)- and Cre(+)-tissues; #3 and #4, Cre(-)- and Cre(+)-isolated hepatocytes. Each sample was hybridized 3×, on 3 separate sectors across the 2 chips, as diagrammed.

**Figure 2.**

Detection of CD74 in cell extracts on Western Blots. (A) *Ikkβ^{F/F}* and *Ikkβ^{Δhep}* mouse livers, and cultured MEFs (each lane from a separate mouse). Lanes: 1 (wildtype MEFs), 2 (*Ikkβ^{-/-}* MEFs), 3 (♂ *Ikkβ^{F/F}* liver), 4 (♂ *Ikkβ^{Δhep}* liver), 5 (♀ *Ikkβ^{F/F}* liver), 6 (♀ *Ikkβ^{Δhep}* liver). Non-specific ~25 kDa and ~55 kDa bands in isotype control panels (right upper and lower) likely reflect non-specific cross-reactions with serum or reagent light and heavy IgG chains. (B) *Ikkβ^{+/+}:Alb-Cre* mouse livers and spleens, and cultured MEFs (each lane from a separate mouse). Lanes: 1 (♂ #1, *Alb-Cre* liver), 2 (♂ #1, *Alb-Cre* spleen), 3 (♂ #2, *Alb-Cre* liver), 4 (♂ #2, *Alb-Cre* spleen), 5 (♂ *Ikkβ^{F/F}* liver), 6 (♂ *Ikkβ^{Δhep}* liver), 7 (*Ikkβ^{-/-}* MEFs), 8 (wildtype MEFs). Loading controls (both panels) showed comparative intensities of 94-96 kDa bands in all lanes.

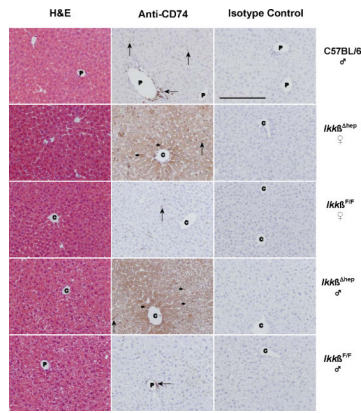
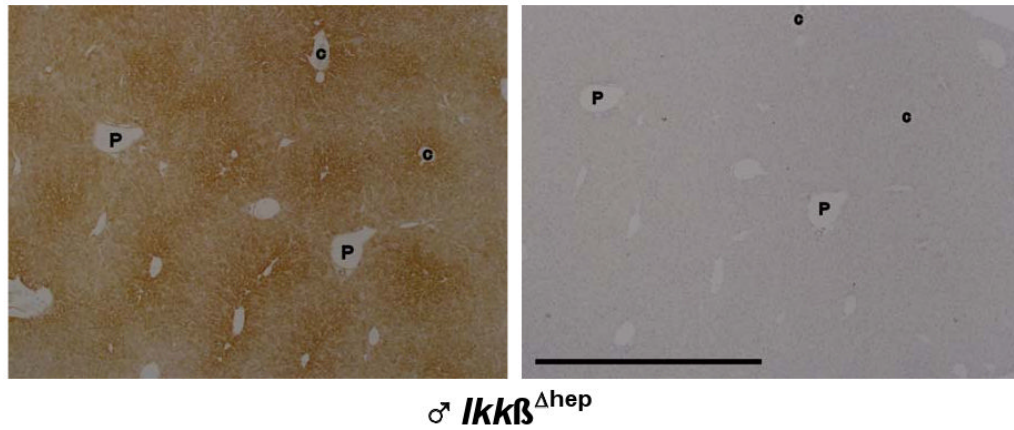


Figure 3.

Histochemical studies of CD74 in livers from C57BL/6 ♂, and *Ikkβ^{F/F}* and *Ikkβ^{Δhep}* ♀ and ♂ mice. Photomicrographs of liver tissue sections stained with H&E, anti-CD74 antibody, or isotype control antibody are shown in the left-, middle-, and right-hand columns, respectively. The sections are from individual C57BL/6 (row 1), *Ikkβ^{Δhep}* ♀ (row 2), *Ikkβ^{F/F}* ♀ (row 3), *Ikkβ^{Δhep}* ♂ (row 4), and *Ikkβ^{F/F}* ♂ (row 5) mice. Annotations indicate hepatocyte membrane (small →) and NPC (large →) staining; C, central vein; P, portal triad. (The unannotated H&E stained *Ikkβ^{Δhep}* ♀ liver section appears to approach a central region.) Specific CD74 staining is present in hepatocytes from *Ikkβ^{Δhep}* mice but not in hepatocytes from C57BL/6 and *Ikkβ^{F/F}* mice. Tissue-specific CD74 staining is not seen in sections treated with isotype control antibody. Objective magnification = 20× (the solid bar, lower left, in the C57BL/6 isotype control panel = 200 μm; the scale bar is identical for experimental panels).

Anti-CD74

Isotype Control

**Figure 4.**

Enriched CD74 staining in *Ikkβ^{Δhep}* hepatocytes in midzonal-to-centrilobular regions. Serial sections from a ♂ *Ikkβ^{Δhep}* liver, stained with either anti-CD74 or isotype control antibodies as described in the text and in Fig. 3, are here placed in register. Low objective magnification (4×) was used to illustrate the zonal gradient of staining intensity. Hepatocytes proximal to central veins (C) are more intensely stained than hepatocytes proximal to portal triads (P). At lower magnification, scattered NPC staining is more difficult to visualize. The few notations are placed within the same vessels of both serial sections to facilitate registration of the two panels. The solid bar, lower left, in the isotype control panel = 1000 μm (the scale bar is identical for the experimental panel).

Table 1

Partial results of microarray profiling: Freshly Isolated Liver Tissues. *

IMMUNE SYSTEM PROCESS				
p = 6.46685868E-28				
Rank	Locus	GenBank Acc.#	Description	E**
2	14961	NM_207105.1	Histocompatibility 2, class II antigen A, beta 1 (H2-Ab1)	-8.86
3	14969	NM_010382.1	Histocompatibility 2, class II antigen E beta (H2-Eb1)	-8.65
4	16149	NM_010545.2	CD74 antigen (invariant polypeptide of major histocompatibility complex)	-8.37
5	14960	NM_010378.2	Histocompatibility 2, class II antigen A, alpha (H2-Aa)	-6.21
6	14963	NM_008199.1	Histocompatibility 2, blastocyst (H2-BI)	+5.72
8	14998	NM_010386.2	Histocompatibility 2, class II, locus DMA (H2-DMa)	-5.11
DEFENSE RESPONSE				
p = 2.07679921E-27				
Rank	Locus	GenBank Acc.#	Description	E**
4	16149	NM_010545.2	CD74 antigen (invariant polypeptide of major histocompatibility complex)	-8.37
6	14963	NM_008199.1	Histocompatibility 2, blastocyst (H2-BI)	+5.72
10	17329	NM_008599	Chemokine (C-X-C motif) ligand 9 (Cxcl9)	-4.97
18	15019	NM_023124	Histocompatibility 2, Q region locus 8 (H2-Q8)	-3.82
20	20210	NM_011315	Serum amyloid A 3 (Saa3)	-3.74
29	55985	NM_018866.1	Chemokine (C-X-C motif) ligand 13 (Cxcl13)	-3.31
30	20304	NM_013653.1	Chemokine (C-C motif) ligand 5 (Ccl5)	-3.29
34	12262	NM_007574.1	Complement component 1, q subcomponent, C chain (C1qc)	-3.08
37	17105	NM_017372	Lysozyme (Lyzs)	-2.9
42	12260	NM_009777.1	Complement component 1, q subcomponent, beta polypeptide (C1qb)	-2.85
43	17069	NM_008529.2	Lymphocyte antigen 6 complex, locus E (Ly6e)	-2.82
53	14127	NM_010185.2	Fc receptor, IgE, high affinity I, gamma polypeptide (Fcer1g)	-2.55
67	24088	NM_011905.2	Toll-like receptor 2 (Tlr2)	-2.31
72	21356	NM_009318.1	TAP binding protein (Tapbp)	-2.29
74	15945	NM_021274.1	Chemokine (C-X-C motif) ligand 10 (Cxcl10)	-2.29
78	17110	NM_013590.2	Lysozyme (Lyzs)	-2.25
82	12505	AK045226	CD44 antigen (Cd44)	-2.22

* Selected expression comparisons between markers from *Ikkβ^{F/F}* and *Ikkβ^{Δhep}* freshly isolated liver tissues are listed; the markers with these comparatively most disparate expression levels are clustered within two functional groups.

** Enrichment, E**, as measured by relative microarray chip hybridization signals, is defined as follows: a negative (-) E value signifies that *Ikkβ^{Δhep}* > *Ikkβ^{F/F}*, and a positive (+) E value signifies that *Ikkβ^{F/F}* > *Ikkβ^{Δhep}* (because the initial comparative chip data were expressed as X-fold enrichment of hybridization markers from *Ikkβ^{F/F}* compared to those from *Ikkβ^{Δhep}* RNA samples).

Table 2

Partial results of microarray profiling: Freshly Isolated Hepatocytes.*

DEFENSE RESPONSE				
p = 1.38089039E-21				
Rank	Locus	GenBank Acc.#	Description	E**
1	16149	NM_010545.2	CD74 antigen (invariant polypeptide of major histocompatibility complex, class II antigen-associated) (Cd74)	-38.31
19	15953	NM_008330.1	Interferon gamma inducible protein 47 (Ifi47)	-7.15
23	15944	NM_008326.1	Immunity-related GTPase family, M (Irgm)	-6.51
24	17329	NM_008599	Chemokine (C-X-C motif) ligand 9 (Cxcl9)	-6.51
27	93671	NM_053094.1	CD163 antigen (Cd163)	+5.7
34	21356	NM_001025313.1	TAP binding protein (Tapbp)	-5.23
45	17105	NM_017372	Lysozyme (Lyzs)	-4.5
53	12505	AK045226	CD44 antigen (Cd44)	-4.25
55	15024	NM_010395.5	Histocompatibility 2, T region locus 10 (H2-T10)	-4.17
64	21354	NM_013683.1	Transporter 1, ATP-binding cassette, sub-family B (MDR/TAP) (Tap1)	-3.96
65	24088	NM_011905.2	Toll-like receptor 2 (Tlr2)	-3.96
66	12260	NM_009777.1	Complement component 1, q subcomponent, beta polypeptide (C1qb)	-3.96
67	12774	NM_009917.2	Chemokine (C-C motif) receptor 5 (Ccr5)	-3.92
69	17110	NM_013590.2	Lysozyme (Lyzs)	-3.87
IMMUNE SYSTEM PROCESS				
p = 1.17768030E-18				
Rank	Locus	GenBank Acc.#	Description	E**
1	16149	NM_010545.2	CD74 antigen (invariant polypeptide of major histocompatibility complex, class II antigen-associated) (Cd74)	-38.31
3	14961	NM_207105.1	Histocompatibility 2, class II antigen A, beta 1 (H2-Ab1)	-22.48
4	14969	NM_010382.1	Histocompatibility 2, class II antigen E beta (H2-Eb1)	-18.24
6	14998	NM_010386	Histocompatibility 2, class II, locus DMA (H2-DMA)	-15.82
7	14960	NM_010378.2	Histocompatibility 2, class II antigen A, alpha (H2-Aa)	-14.39
8	21822	NM_011579.2	T-cell specific GTPase (Tgtp)	-13.26
9	14468	NM_010259.1	Guanylate nucleotide binding protein 1 (Gbp1)	-11.94
11	14999	NM_010387.2	Histocompatibility 2, class II, locus Mb1 (H2-DMb1)	-10.6
13	15000	NM_010388	Histocompatibility 2, class II, locus Mb2 (H2-DMb2)	-9.36
14	55932	NM_018734.2	Guanylate nucleotide binding protein 3 (Gbp3)	-8.96
20	14469	NM_010260.1	Guanylate nucleotide binding protein 2 (Gbp2)	-7.02
24	17329	NM_008599	Chemokine (C-X-C motif) ligand 9 (Cxcl9)	-6.51
30	60533	NM_021893.2	CD274 antigen (Cd274)	-5.54
33	16912	NM_013585.1	Proteasome (prosome, macropain) subunit, beta type 9 (large multifunctional peptidase 2) (Psmb9)	-5.31
34	21356	NM_001025313.1	TAP binding protein (Tapbp)	-5.23
49	16913	NM_010724	Proteasome (prosome, macropain) subunit, beta type 8 (large multifunctional peptidase 7) (Psmb8)	-4.38
56	16362	NM_008390.1	Interferon regulatory factor 1 (Irf1)	-4.16

IMMUNE SYSTEM PROCESS
p = 1.17768030E-18

Rank	Locus	GenBank Acc.#	Description	E**
64	21354	NM_013683.1	Transporter 1, ATP-binding cassette, sub-family B (MDR/TAP) (Tap1)	-3.96
65	24088	NM_011905.2	Toll-like receptor 2 (Tlr2)	-3.96

* Selected expression comparisons between markers from *Ikkβ^{F/F}* and *Ikkβ^{Δhep}* freshly isolated hepatocytes are listed; the markers with these comparatively most disparate expression levels are clustered within two functional groups.

** Enrichment, E**, as measured by relative microarray chip hybridization signals, is defined as follows: a negative (-) E value signifies that *Ikkβ^{Δhep}* > *Ikkβ^{F/F}*, and a positive (+) E value signifies that *Ikkβ^{F/F}* > *Ikkβ^{Δhep}* (because the initial comparative chip data were expressed as X-fold enrichment of hybridization markers from *Ikkβ^{F/F}* compared to those from *Ikkβ^{Δhep}* RNA samples).

Table 3

Microarray profiling: Partial comparisons between mouse embryo fibroblasts (MEFs, *Ikkβ^{-/-}* vs. wild type MEFs) and freshly isolated hepatocytes (*Ikkβ^{Δhep}* vs. *Ikkβ^{F/F}*).

Gene	MEFs (<i>Ikkβ^{-/-}</i> vs. wt)	Hepatocytes (<i>Ikkβ^{Δhep}</i> vs. <i>Ikkβ^{F/F}</i>)	GenBank Acc. #	Function
X-fold enrichment*				
CARP	+156.3	-1.21	AF041847	Cardiac ankyrin repeat protein, binding to myopalladin
Versican	+9.7	NR	D45889	Anti-cell adhesive molecules
α-Actin	+2.6	+1.28	X13297	Cytoskeleton, stress fibers
Prothymosin β4	+2.34	-1.98	U38967	Prevents actin polymerization
S100A4	+2.2	NR	M36579	Tumor metastasis, calcium-binding protein
Tropomyosin 2	+2.0	-1.47	M22479	Actin-binding protein
IGFBP2	-134	-1.79	X81580	Inhibitor of cell mitogenesis
TIMP-2	-5.8	-2.32	X62622	Inhibitor of matrix metalloproteinases
TIMP-3	-4.0	-1.99	U26437	Inhibitor of matrix metalloproteinases
VCAM	-2.9	+5.62	M84487	Vascular cell adhesion molecule
Integrin β5	-2.0	-1.2	AF022110	Cell adhesion

X-fold enrichment values for MEFs were taken from Chen et al., 2006. The X-fold enrichment value is here in Table 3 defined as the relative comparison of RNA hybridization expression of MEF *Ikkβ^{-/-}* to MEF *Ikkβ^{+/+}*, or of *Ikkβ^{Δhep}* to *Ikkβ^{F/F}* such that a positive (+) value signifies that MEF *Ikkβ^{-/-}* > MEF *Ikkβ^{+/+}*, or that *Ikkβ^{Δhep}* > *Ikkβ^{F/F}*; and, a negative (-) value signifies that MEF *Ikkβ^{+/+}* > MEF *Ikkβ^{-/-}*, or that *Ikkβ^{F/F}* > *Ikkβ^{Δhep}*. Note that this definition is here the reverse of that in Tables 1 and 2, in order to establish congruence with the E values previously published for the MEF *Ikkβ^{-/-}* and *Ikkβ^{+/+}* pair.